Fast Procedure for Reconstruction of Full-Atom Protein Models from Reduced Representations

PIOTR ROTKIEWICZ,[1] JEFFREY SKOLNICK[2]

[1]*Burnham Institute for Medical Research, 10901 N. Torrey Pines Road, La Jolla, California 92037*
[2]*Center for the Study of Systems Biology, Georgia Institute of Technology, 250, 14th Street NW, Atlanta, Georgia 30318*

Abstract: We introduce PULCHRA, a fast and robust method for the reconstruction of full-atom protein models starting from a reduced protein representation. The algorithm is particularly suitable as an intermediate step between coarse-grained model-based structure prediction and applications requiring an all-atom structure, such as molecular dynamics, protein-ligand docking, structure-based function prediction, or assessment of quality of the predicted structure. The accuracy of the method was tested on a set of high-resolution crystallographic structures as well as on a set of low-resolution protein decoys generated by a protein structure prediction algorithm TASSER. The method is implemented as a standalone program that is available for download from http://cssb.biology.gatech.edu/skolnick/files/PULCHRA.

© 2008 Wiley Periodicals, Inc.   J Comput Chem 29: 1460–1465, 2008

Key words: reduced protein representation; protein structure prediction; side chain and backbone reconstruction; protein model refinement

Introduction

To efficiently sample protein-conformational space, protein structure prediction algorithms often use a reduced protein representation. For example, instead of calculating interactions between all protein atoms, every amino acid can be represented by a single center of interaction (e.g., positioned on a side-chain center of mass).[1] Thus, the amount of calculations necessary to calculate the energy of the system can be dramatically reduced. Although the reduced models are necessary to efficiently search conformational space, fine-detailed all-atom models are often essential for subsequent structural studies. The full-atom representation is required for many applications, such as protein function analysis, virtual ligand screening, prediction of protein–protein interactions, and assessment of structure quality.[2] Therefore, following assembly of an approximate fold, the reduced models need to be translated into detailed atomic models for later analysis.

The idea behind this work is to develop a fast and complete procedure for the conversion of reduced protein models into all-atom structures suitable for subsequent optimization using molecular mechanics force fields. Reduced representations can include α-carbon only representation, a side-chain rotamer center of mass, an α-carbon and side-chain rotamer center of mass representation, or other centers of interactions (e.g., Cβ atoms). The procedure should avoid creating structural errors that may render the full-

atom model inappropriate for further molecular mechanics optimization. For example, most molecular mechanics force fields cannot fix the problem of "punched" aromatic rings, because they lack the ability to break covalent bonds. Additionally, the procedure should take into consideration the common inaccuracies of the input models, for instance, distorted α-carbon geometries. Such distortions are often present in structures derived from clustering algorithms where the cluster centroid, which, on average, tends to be the most accurate in terms of the global root mean square deviation (RMSD) from native,[3] is used. However, the resulting Cα virtual bond distances and angles can be unphysical and need to be brought back to a native range.

Here, we present a method named PULCHRA ("Protein Chain Reconstruction Algorithm") for the reconstruction of full-atom protein models. We have implemented the procedure as a standalone program written in C programming language. PULCHRA reads atom coordinates in Protein Data Bank (PDB) format and outputs full-atom PDB files. Typically, the reconstruction

process takes about half a second for a 300 amino acid long protein. The program is a single executable, and it does not require any external data files.* The algorithm is not only fast but also allows for different types of input protein model representation, multichain models, or chain breaks. Additionally, the user is allowed to largely control the reconstruction procedure because most of the algorithm parts can be switched off. The current program was developed independently from our previously published approach.[4]

Methods

The method developed in this work consists of several steps. First, input α-carbons are optimized using a simple force field and a steepest-descent minimization. Subsequently, the backbone nitrogen and carbonyl group atoms are reconstructed. The reconstructed backbone can be optimized to improve the hydrogen bond pattern. Next, the amino acid side-chain heavy atoms are placed on the backbone. Then, the side chains are optimized to minimize possible atom–atom clashes. Finally, hydrogen atoms are added to the protein model. Each of these steps is optional and can be omitted. For example, it is not necessary to rebuild the backbone atoms before the side chains are placed.

The statistics for the backbone and side-chain rotamer libraries were gathered from a representative list of 1351 high-quality crystallographic protein structures with resolution better than 2.0 Å, clustered at a level of 35% sequence identity.

Optimization of α-Carbon Positions

The positions of the α-carbon atoms are optimized using a steepest-descent gradient minimization algorithm and a simple harmonic potential. The potential (V) consists of the following terms: pairwise Cα—Cα distances, Cα—Cα—Cα virtual bond angles, Cα excluded volume, and the deviation from the initial positions [eq. (1)]:

$$V = w_1 \sum_{i=1}^{N-1} (d_{i,i+1} - d_0)^2 + w_2 \sum_{i=1}^{N-2} (\theta_{i,i+1,i+2} - \theta_0)^2$$
$$+ w_3 \sum_{i=1}^{N-2} \sum_{j=i+2}^{N} (d_{i,j} - d_{ex})^2 + w_4 \sum_{i=1}^{N} (d_{i,i_0} - d_u)^2 \quad (1)$$

where N is the number of Cα atoms; w_1, w_2, w_3, and w_4 are weights of the corresponding potential terms; $d_{i,i+1}$ is the distance between the ith and $i + 1$th Cα atoms and d_0 is the equilibrium Cα—Cα distance equal to 3.8 Å; $\theta_{i,i+1,i+2}$ is the virtual bond angle involving the ith, $i + 1$th, and $i + 2$th Cα atoms; θ_0 is the equilibrium angle, $\theta_0 = 70°$ if $\theta_{i,i+1,i+2} < 70°$, $\theta_0 = 150°$ if $\theta_{i,i+1,i+2} > 150°$, or $\theta_0 = \theta_{i,i+1,i+2}$ otherwise; d_{ex} is equal to 4 Å if $d_{i,j} < 4$ Å or $d_{ex} = d_{i,j}$ otherwise; $d_{i,i0}$ is the distance between the actual and initial α-carbon positions, and if $d_{i,i0}$ is smaller than maximum allowed displacement threshold, d_u

(default value: 0.5 Å), then $d_{i,i0} = d_u$. The potential term weights, w_1, w_2, w_3, and w_4, were optimized by hand and are equal to 1.0, 2.0, 10.0, and 0.5, respectively.

Two special cases need to be treated differently. The first is cis-proline, in which an equilibrium Cα—Cα distance is equal to 2.9 Å. The presence of a cis-proline can be determined from the initial Cα coordinates or can be explicitly defined by the user. The second case is the presence of chain breaks. The chain is considered broken if a distance between two consecutive Cα atoms is larger than a certain threshold (4.5 Å, by default). In such a case, distance and angle restraints are not calculated for the residues involved in the chain break [weights w_1 and w_2 in eq. (1) are equal to 0].

After performing a steepest-descent minimization procedure ($dV/dr \rightarrow 0$), the resulting structure has Cα—Cα distances and Cα—Cα—Cα angles close to native values, with the displacements from the initial positions controlled by the parameter d_u. Typically, less than 100 minimization steps are necessary for the procedure to converge. The optimized structure is always a compromise between local geometric correctness and the deviation from the initial structure. Sometimes, especially in the case of a heavily distorted input chain, the minimization procedure does not converge, or the optimized model still exhibits irregularities. When such an event occurs, it is possible to restart the minimization from a random or fully extended chain conformation rather than from the initial coordinates.

If no α-carbon coordinates are provided on input, their positions can be approximated from the side-chain centers of mass [eq. (2)]:

$$r_i = \frac{s_{i-1} + s_i + s_{i+1}}{3} \quad (2)$$

and rescaled according to the average distance between the Cα and the side-chain center of mass, CM [eq. (3)]:

$$r_i = s_i + \frac{R_i}{|r_i - s_i|} (r_i - s_i) \quad (3)$$

In eqs. (2) and (3), r_i is the position of the ith Cα, s_i is the position of the ith side-chain center of mass, R_i is an average statistical Cα-CM distance for an amino acid at position i, $|r_i - s_i|$ is the distance between the ith amino acid Cα atom and the center of mass of its rotamer. Subsequently, the positions of the approximated Cα carbons are optimized, as described earlier.

Backbone Reconstruction

The backbone reconstruction method is based on a refined version of an algorithm proposed by Milik et al.[5] The procedure requires four consecutive α-carbon positions rebuild the peptide bond atoms between the two central α-carbons. The procedure works as follows: first, the distances between the first and third (r_{13}), second and fourth (r_{24}), and first and fourth (r_{14}) α-carbon atoms are calculated (Fig. 1). Additionally, the sign of r_{14} corresponds to the local chirality of the chain. The native distributions of these distances are divided into a number of bins: 10 bins ranging from 4.5 to 7.5 Å for r_{13} and r_{24}, and 75 bins rang-
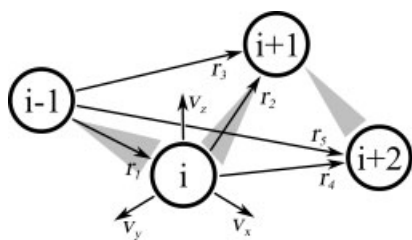
Figure 1. Frame of reference used for reconstruction of the backbone and side-chain atoms. The vectors r_1, r_2, and r_3 are used to construct a local system of coordinates, v_x, v_y, and v_z, according to eqs. 4(a–c). The local system of coordinates is used to rebuild the backbone plate between the *i*th and *i* + 1th α-carbons and the side-chain atoms of the *i*th α-carbon. The distances r_3, r_4, and r_5 are used to choose a proper side chain and peptide plate conformation from a fragment library.

ing from −11 to 11 Å for r_{14}. Next, each of the calculated distances is assigned to one of the bins. Subsequently, the bins are used to choose a proper fragment from a backbone fragment library (N, C, and O peptide bond atoms). Then, a local system of coordinates for every Cα atom is calculated, and the backbone atoms are transformed to the local coordinates and added to the chain. The local system of coordinates is defined by three orthogonal axes v_x, v_y, v_z [eq. (4)]:

$$v_x = \frac{r_{13}}{|r_{13}|} \tag{4a}$$

$$v_y = \frac{r_{23} \times r_{12}}{|r_{23} \times r_{12}|} \tag{4b}$$

$$v_z = v_x \times v_y \tag{4c}$$

where r_{xy} is a vector connecting the positions of the *x*- and *y*-α-carbon atoms.

Backbone Optimization

Often, in the reconstructed backbone, its hydrogen bond pattern is distorted. The positions of the backbone atoms can be adjusted to optimize this pattern, especially in the regular secondary structure regions (α-helices and β-sheets). This simple optimization procedure calculates the hydrogen bond energy of every peptide plate with respect to its spatially closest neighbor using the hydrogen bond definition found in the DSSP program.[6] The hydrogen bond energy of a hydrogen bond C—O...H—N is calculated according to a following formula:

$$E_{HB} = 332 q_1 q_2 \left(\frac{1}{r_{ON}} + \frac{1}{r_{CH}} - \frac{1}{r_{OH}} - \frac{1}{r_{CN}} \right) \tag{5}$$

where $q_1 = 0.42e$ and $q_2 = 0.20e$, with *e* being the electron charge unit, r_{XY} the distance between atoms *X* and *Y* in

angstroms, and E_{HB} the energy in kcal/mole. As the energy computation requires explicitly defined peptide bond hydrogen atoms, the hydrogen atoms positions are reconstructed at this stage.

For every consecutive Cα—Cα pair, the peptide bond atoms are rotated along the Cα—Cα virtual bonds within a (−10°, 10°) range using an angle step of 1° (Fig. 2). The energy is calculated at each step, and if a better peptide plate orientation is found, then the old orientation is replaced by the new one. This procedure is repeated for every peptide plate.

Side-Chain Reconstruction

Even very simple side-chain rebuilding algorithms can generate reasonable models comparable with results of more elaborate methods, as suggested elsewhere.[7] The accuracy of side-chain reconstruction can be significantly higher if positions of side-chain centers of mass are present in the input data.[8] Our side-chain reconstruction procedure uses the same reference frame (local system of coordinates and set of distances) as the backbone reconstruction procedure (Fig. 1). Therefore, both reconstruction procedures can be used independently, and it is not necessary to rebuild the backbone atoms before the side chains, contrary to most other side-chain reconstruction methods. For every combination of calculated distance bins, there is a list of possible side-chain conformations sorted according to the probability of occurrence in the PDB.[9] If no side-chain center of mass information is given on input, the most probable conformer is used. Otherwise, the procedure reconstructs the side-chain closest to the given side-chain center of mass.

Side-Chain Optimization

After the side chains are reconstructed, their positions can be fine tuned to avoid possible heavy-atom clashes, where preserving the side chain–side chain packing. Two atoms are considered clashed if the distance between them is lower than 2 Å. The optimization procedure works as follows: first, the side-chain rotamers are sorted according to the number of excluded volume violations and processed in this order. Next, the rotamer library is searched for less-probable side-chain conformations that match the previously calculated Cα frame of reference as closely

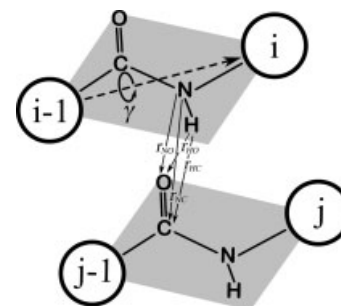**Figure 2.** Hydrogen bond pattern optimization procedure. The peptide bond atoms are rotated around a virtual Cα—Cα bond, whereas the bond energy is calculated according to the DSSP formula (Eq. 5). The optimal conformation within a (−10°, 10°) range of the γ angle is stored.
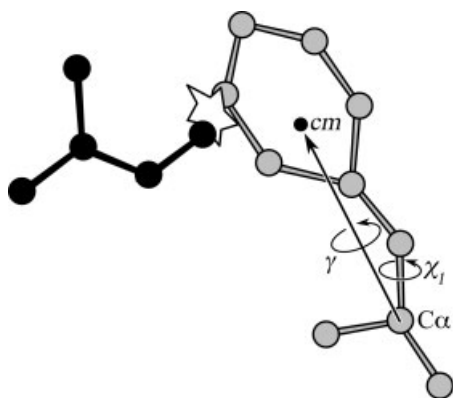
Figure 3. Optimization of side-chain positions. The side-chain is rotated by an angle γ around a Cα—CM vector until the total number of clashes with other heavy atoms is minimized. Additionally, the χ_1 angle is calculated and tested against the allowed range to exclude nonphysical side-chain conformations.

as possible. The previous rotamer is replaced by a new one, and the excluded volume violations are checked again. This process is repeated iteratively until all clashes are removed, or a certain number of iterations are reached (default: 100 iterations). If the clashes are still present, the side chain is rotated around a virtual Cα—CM bond (Fig. 3). This simple procedure works surprisingly well. Usually, over 95% of the initial clashes are removed, whereas the pattern of side chain–side chain contacts remains very similar (over 85% of the contacts are preserved).

The problem of punched aromatic rings due to penetration of the aromatic ring by other side-chain heavy atoms is a more serious issue (Fig. 4). This kind of nonphysical arrangement cannot be easily solved using molecular mechanics minimization; therefore, such models are often useless in subsequent molecular dynamics simulations. Similarly as mentioned earlier, the rotamer library is scanned to find closest rotamer conformation that avoids the punch. Our algorithm tries to minimize the possibility of punched ring occurrence, even at the cost of excluded volume violations. If, despite reaching a preset number of iterations, the problem cannot be fixed—the optimization is stopped and the problem is reported to the user.

Additionally, the structure is checked for possible chirality errors (occurrence of D amino acid conformations). To perform this check, the improper dihedral angle involving the Cα—N—C—Cβ atoms is calculated. In L-amino acid conformations, this angle is right handed and is close to $34°$. In D-amino acids, the angle value is negative (the angle is left handed). If a D-amino acid occurs, the side chain is flipped over the N—Cα—C plane, so that the amino acid conformation is inverted.

Hydrogen Atoms Reconstruction

In the final step, hydrogen atoms can optionally be added to the full-atom representation. The positions of the hydrogen atoms are calculated according to the heavy atom types and their

hybridization states. Although possible clashes with heavy atoms are not checked at this stage, a subsequent molecular minimization procedure usually solves this problem whenever it occurs.

Results

We compared the performance of PULCHRA with two popular side-chain reconstruction programs, SCWRL 3.0[10] and SCATD 1.0.[11] Both programs use a backbone-dependent rotamer library,[12] but the SCATD algorithm is faster and less prone to problems with inaccurate input structures. In contrast to PUL-CHRA, both algorithms expect an all-atom backbone structure on input. Also, the programs do not attempt to regularize the backbone geometry nor solve punched rings. Additionally, we compared our results with the results of a similar method published previously, available as a "rebuild.pl" program included in the multiscale modeling tools for structural biology (MMTSB) package.[4,13]

The overall accuracy of heavy-atom reconstruction was assessed using 30 high-quality crystallographic structures of resolution better than 1.0 Å, extracted from a recent edition of representative protein structure database clustered at 25% sequence identity level.[14] Complete backbone coordinates were taken from the native structures. After reconstruction, we calculated the RMSD of the best superposition of all heavy atoms between the reconstructed model and the native structure (Table 1). When the Cα coordinates were used as input, the average all-atom RMSD was equal to 1.53 Å. When information about side-chain centers of mass was added, the all heavy-atom RMSD from the native structure decreased to 0.97 Å. The MMTSB tool requires that the center of mass coordinates be present in the input files (it does not handle Cα-only structures). When using this information, the MMTSB method can generate
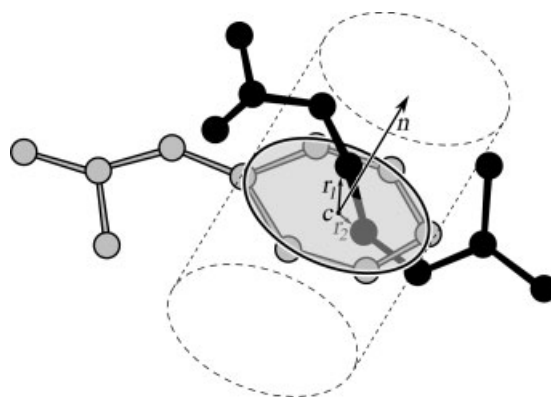
Figure 4. Example of a punched ring. The arginine side chain is threaded through a phenylalanine aromatic ring. The n vector is the ring plane normal, and r_1 and r_2 are vectors connecting the ring center, c, with the Xγ and Cδ atoms of an arginine side chain. The signs of scalar products of n and r vectors determine the positions of the atoms with respect to the ring plane. If two atoms are positioned on alternate sides of the ring, within a certain distance from a ring center, the ring is considered to be punched by the side chain.

Table 1. Comparison of Side Chains Reconstruction Quality Between PULCHRA, MMTSB, SCWRL, and SCATD

Protein PDB code	Resolution (Å)	Length (AA)	All-atom RMSD (starting from a native backbone)				
			PULCHRA using Cα only	PULCHRA using Cα + CM	MMTSB using Cα + CM	SCWRL	SCATD
1ejgA	0.54	46	0.948	0.766	0.899	0.862	1.377
1et1A	0.90	34	1.803	0.838	0.921	1.675	1.765
1f9yA	0.89	158	1.655	0.995	0.940	1.152	1.311
1g66A	0.90	207	1.350	1.008	0.644	0.910	0.914
1ix9A	0.90	205	1.647	1.087	0.844	1.170	1.328
1iqzA	0.92	81	1.378	0.806	0.750	1.060	1.038
1iuaA	0.80	83	1.303	0.952	0.728	0.918	0.965
1lugA	0.95	259	1.615	1.120	0.803	1.109	1.226
1m40A	0.85	263	1.621	1.095	0.849	1.296	1.365
1mc2A	0.85	122	1.660	1.060	0.755	1.247	1.318
1mj5A	0.95	297	1.718	1.099	0.808	1.170	1.433
1n4wA	0.92	498	1.534	1.001	0.741	1.164	1.268
1n55A	0.83	249	1.515	0.831	0.729	1.035	1.073
1nwzA	0.82	125	1.619	0.944	0.830	1.173	1.319
1ok0A	0.93	74	1.518	0.958	0.787	1.226	1.257
1p9gA	0.84	41	1.472	1.136	0.884	1.113	1.220
1pjxA	0.85	314	1.643	1.062	0.858	1.085	1.133
1pq7A	0.80	224	1.404	0.798	0.706	0.787	0.956
1r6jA	0.73	82	1.325	0.861	0.984	0.859	0.925
1rtqA	0.95	291	1.536	0.839	0.738	1.126	1.049
1ucsA	0.62	64	1.545	1.023	0.777	0.872	0.967
1us0A	0.66	313	1.742	0.992	0.708	1.220	1.260
1v6pA	0.87	62	1.523	1.047	1.140	1.360	1.467
1vyrA	0.90	363	1.631	1.012	0.735	1.006	1.132
1w0nA	0.80	120	1.455	0.912	0.843	1.008	0.979
1wy3A	0.95	35	1.897	1.236	1.298	1.458	1.718
1x8qA	0.85	184	1.621	0.993	0.837	1.203	1.343
2bt9C	0.94	88	1.410	1.022	0.702	1.052	1.309
2pvbA	0.91	107	1.477	0.749	0.676	1.075	1.182
7a3hA	0.95	300	1.425	0.715	0.729	0.974	1.073
Average			1.533	0.965	0.820	1.112	1.222

even more accurate models with an average all-atom RMSD from native equal to 0.82 Å. The all-atom RMSD from the native conformation calculated using SCWRL and SCATD programs was equal to 1.11 and 1.22 Å, respectively. PULCHRA was the fastest out of all four programs, with an average reconstruction time per protein equal to 0.8 s, compared to 1.0, 2.4, and 1.3 s in case of MMTSB, SCWRL, and SCATD, respectively.

Separately, we tested backbone reconstruction accuracy by PULCHRA. The average RMSD from native structures calculated over the reconstructed backbone atoms only was equal to 0.50 Å. Subsequent application of a backbone optimization procedure slightly improved the backbone RMSD by 0.007 Å, whereas average DSSP hydrogen bond energy dropped by 29.4 kcal/mol (Table 2).

To check our method in a real-life application, we performed a test on 500 decoy structures randomly chosen from a genomic-scale Monte Carlo protein structure prediction benchmark.[3] These structures are simulation models closest to average cluster centroids, and their local geometry is often seriously distorted. The RMSD from the native structures ranged from 1.1 to 25 Å. The reconstructed structures with optimized Cα positions have slightly higher RMSD to native structures than the initial decoy structures. On average, the difference is equal to 0.18 Å. However, in contrast to the initial decoys, local distances and angles in the optimized structures are in the range of the physically acceptable values. After optimizing α-carbon positions and rebuilding the backbone by PULCHRA, the models were subject to side-chain reconstruction using the four programs. The reconstruction accuracy of all four methods was comparable: the average all-atom RMSD from the native, calculated over the reconstructed decoy set, was equal to 10.18, 10.26, 10.21, and 9.89 Å, for PULCHRA, MMTSB, SCATD, and SCWRL, respectively. PULCHRA calculations took 1.3 s per protein, MMTSB required 2.0 s per protein, whereas SCATD calculations took 2.4 s, and SCWRL took 28.8 s. The speed difference between PULCHRA and MMTSB is mostly related to the Cα

Table 2. Quality of Backbone Reconstruction and Optimization Tested on 30 High-Resolution Native Structures

Protein PDB code	PULCHRA backbone RMSD before optimization (Å)	PULCHRA backbone RMSD after optimization (Å)	DSSP energy change during backbone optimization (kcal/mol)
1ejgA	0.470	0.466	−14.3
1et1A	0.310	0.337	−12.6
1f9yA	0.461	0.462	−16.2
1g66A	0.543	0.535	−3.3
1ix9A	0.494	0.490	−11.3
1iqzA	0.471	0.469	−21.4
1iuaA	0.551	0.525	−9.8
1lugA	0.518	0.511	−61.2
1m40A	0.475	0.474	−11.4
1mc2A	0.544	0.546	−9.3
1mj5A	0.585	0.580	−10.9
1n4wA	0.493	0.487	−36.8
1n55A	0.409	0.404	−52.0
1nwzA	0.485	0.467	−62.3
1ok0A	0.494	0.468	−47.5
1p9gA	0.535	0.516	−65.4
1pjxA	0.579	0.567	−56.5
1pq7A	0.543	0.536	−45.5
1r6jA	0.465	0.464	−39.8
1rtqA	0.435	0.429	−4.33
1ucsA	0.574	0.546	−39.5
1us0A	0.401	0.406	−39.8
1v6pA	0.578	0.553	−50.2
1vyrA	0.507	0.505	−50.2
1w0nA	0.542	0.538	−24.9
1wy3A	0.663	0.663	−28.2
1x8qA	0.458	0.445	−21.0
2bt9C	0.627	0.624	−13.9
2pvbA	0.388	0.381	−8.1
7a3hA	0.428	0.424	−17.0
Average	0.501	0.494	−29.4

optimization stage. In case of SCWRL, sometimes the calculations took a very long time; therefore, the program was stopped after running for more than 1 min. That was the case for 37 of 500 decoys. Of 500 reconstructed decoys, PULCHRA generated six cases of not fixed punched rings or excluded volume violations in the output models. The MMTSB "rebuild.pl" tool generated 40 cases of the punched rings, SCWRL generated 70 cases, and SCATD generated 130 such cases. The detected problems were usually related to side chain and backbone overlaps in seriously distorted parts of the input chains.

Conclusions

Reconstruction of an all-atom representation of a predicted protein's structure is an important part of the protein structure modeling pipeline. Here, we introduce PULCHRA, a fast and robust tool for the reconstruction of full-atom models. We have demonstrated that the program can handle even seriously distorted input structures, still being able to generate reasonable full-atom models. A similar technique, implemented as a part of the MMTSB toolkit, was published before.[4] Although the reconstruction accuracy is similar in case of these two methods, PULCHRA is faster, more robust, and less frequently generates nonfixable errors in the reconstructed models. The quality of the rebuilt models is satisfactory, and the reconstructed structures can be directly used for further refinement with molecular mechanics programs. The program can handle incomplete structures that have gaps in the Cα chain. If information about the side-chain centers of mass is available, the reconstruction accuracy increases significantly. In addition, PULCHRA can process entire molecular simulation trajectories (in a form of multimodel PDB files) as well as protein quaternary structures (multichain models). Also, the program preserves input information (such as atom numbering, PDB chain labels, or any pre-existing atom coordinates). The calculations can be speeded up by switching off certain parts of the algorithm. For example, disabling the initial Cα position optimization routine reduces the computation time by 20–50%, depending on the degree of distortion of the initial coordinates. PULCHRA is a compact, single-executable program; it does not depend on external tools or data libraries, and therefore it can be easily incorporated into existing modeling protocols. PULCHRA was successfully used as a part of a structure-modeling pipeline during the CASP7 experiment.[1]

References

1. Zhou, H.; Pandit, S. B.; Lee, S. Y.; Borreguero, J.; Chen, H.; Wroblewska, L.; Skolnick, J. Proteins: Struct Funct Genet 2007, 69, 90.
2. Wroblewska, L.; Skolnick, J. J Comput Chem 2007, 28, 2059.
3. Zhang, Y.; Skolnick, J. Proc Natl Acad Sci USA 2004, 101, 7594.
4. Feig, M.; Rotkiewicz, P.; Kolinski, A.; Skolnick, J.; Brooks, C. L., III. Proteins: Struct Funct Genet 2000, 41, 86.
5. Milik, M.; Kolinski, A.; Skolnick, J. J Comput Chem 1997, 18, 80.
6. Kabsch, W.; Sander, C. Biopolymers 1983, 22, 2577.
7. Samudrala, R.; Huang, S. E.; Koehl, P.; Levitt, M. Protein Eng 2000, 13, 453.
8. Kazmierkiewicz, R.; Liwo, A.; Scheraga, H. A. Biophys Chem 2003, 100, 261.
9. Berman, H. M.; Westbrook, J.; Feng, Z.; Gilliland, G.; Bhat, T. N.; Weissig, H.; Shindyalov, I. N.; Bourne, P. E. Nucleic Acids Res 2000, 28, 235.
10. Canutescu, A. A.; Shelenkov, A. A.; Dunbrack, R. L. J. Protein Science 2003, 12, 2001.
11. Xu, J. Lecture Notes Comput Sci 2005, 3500, 423.
12. Dunbrack, R. L. J.; Karplus, M. J Mol Biol 1993, 230, 543.
13. Feig, M.; Karanicolas, J. L.; Brooks, C. L., III. J Mol Graph Model 2004, 22, 377.
14. Hobohm, U.; Sander, C. Protein Sci 1994, 3, 522.